Mechanical Properties of Electron Beam Welds of Centrifugal Casting Steel Plates [†]

Yoshiaki ARATA*, Michio TOMIE**, Hisakatsu NISHIHARA***, Takao MIHARA***
and Shinichi KURODA****

Abstract

A horizontal full penetration welding of centrifugal casting steel plates up to 50 mm thickness for 50 kg/mm² class welded structure was conducted by using horizontal electron beam subjected to 90° deflection and a sound weld bead of very narrow width and without internal defects could be obtained. Charpy specimens of different shapes were sampled from the welded zones of one pass full penetration welding with varying welding heat input and the properties were investigated by impact test to study toughness of the welded zones. From the relationship between brittleness fracture transition temperature of the specimen fracture after Charpy impact test and welding heat input, relative toughness was evaluated to verify that the toughness of the welded zones of this material is improved by low heat input welding.

KEY WORDS:: (Electron Beam Welding) (Horizontal EB Welding) (Centrifugal Casting Steel) (Charpy Impact Test) (Crystallinity) (Toughness Evaluation)

1. Introduction

Centrifugal casting steel plates for 50 kg/mm² welded structure are popularly used at present for building columns and others and the application is expanding lately to large sized off shore and land structures.

A highly efficient welding of high grade is demanded for this heavy wall material and a number of studies have been conducted.

To thick plates, a welding method of narrower weld metals of the weld joint and the heat affected zones (HAZ) than that of ordinary multiple layer arc welding and with less thermal deformation and less heat input will be effective, particularly electron beam welding which can form weld beads of deep penetration by one pass.

In view of the above the authors studied the conditions of horizontal position full penetration welding which can produce weld zones of narrow bead width and without any defects to this material by electron beam welding method.

As a result, it turned out that welding of no internal defects is possible up to 100 mm plate thickness[1].

At the performance tests of the weld joints obtained, however, the result of the impact test was even lower than the JIS standard of the base metal (2.8kg-m: 0°C) although the results of tensile strength and bending tests were favourable. The poor result of impact test means low toughness[2),3),4)]. In the study for relative evaluation of

toughness of steel weld zone by electron beam welding, it is indicated that welding heat input is a major factor for toughness. However, no investigations and evaluations have been made systematically in most cases.

In this study, therefore, the metal structures of weld zones were investigated while changing heat input. The toughness was also checked by impact test to obtain some guidance for toughness improvement.

2. Material used, electron beam welder and test method

2.1 Material used

Steel plates of 22 mm and 50 mm thickness were cut from a centrifugally cast steel pipe for welded structure of 50 kg/mm² class (JIS G5201 SCW50-CF equivalent, Kubota Standard SMK 50) and were used for the test. The chemical composition of the material is shown in **Table 1**.

Figure 1 shows the position on the cast steel pipe from which the material plates were out.

The mechanical properties of the material are 50 kgf/mm² tensile strength, and 2.8 kg-m (0°C) and higher of

Table 1 Chemical composition of material used.

(wt %)

	C	Si	Mn	P	S	Ni	Cr	V	O	N	Ceq.
SMK–50	0.16	0.34	0.95	0.018	0.015	0.04	0.16	0.07	0.0037	0.013	0.333

Ceq. = C + 1/24·Si + 1/6·Mn
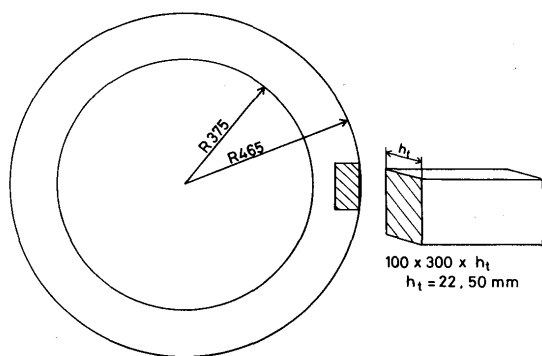Thickness : h_t = 22 , 50 (mm)
(JIS G 5201 SCW 50-CF)

Fig. 1 Extraction of material from casting pipe.

Charpy impact value at standard 2 mmV-notch test piece.

2.2 Electron beam welder and welding method

The electron beam welder used for this test is a high vacuum type with 110 kW maximum beam output and 100 kV beam voltage developed by Arata Laboratory[5].

As shown in **Fig. 2**, the vertical electron beam from a gun was deflected by 90° with a beam deflector placed in the welding chamber of 10^{-4} Torr vacuum to produce horizontal beam, and one pass full penetration bead welding was carried out at horizontal position. To prevent defects at the weld zones, low frequency oscillation (fx = 10 to 100 Hz) was applied to the electron beam in the weld line direction (X-direction in Fig. 2).
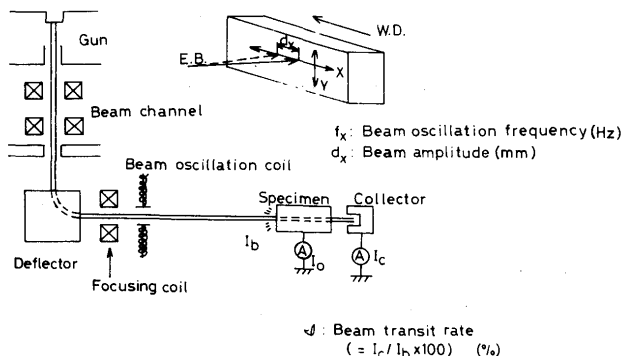

Fig. 2 Schematic diagram of horizontal position welding method.

2.3 Observation of weld zone structure and hardness measurement

For structure observation, an optical microscope and a scanning type electron microscope (SEM) were used.

After electrolytic polishing (30 V-6 sec.) with chromic acid-acetic acid solution, the specimens were etched with solution of 1 cc HNO_3 + 1g picric acid + slight benzalconium chloride + 100 cc amil alcohol.

Particularly for observation of M-A constituent, electrolytic etching (5V-30 sec.) by sodium hydroxide solution (25 g NaOH + 5 g picric acid + 100 cc H_2O) which dissolves carbide was applied in addition to the elec-

trolytic etching (4V − 5 sec.) by EDTA solution (5 g EDTA + 0.5 NaF + 100 cc H_2O) which etches preferentially ferrite structure.

The hardness was tested at 10 kg load with a Vickers hardness tester.

2.4 Shapes of Charpy specimens and sampled position

Figure 3 shows the shapes of three kinds of test pieces used for the Charpy test.

Fig. 3(a) is the standard 2 mmV-notch test piece specified in JIS Z 2202 as No. 4 test piece, Fig. 3(b) shows the shape of 5 mmV-notch test piece, and Fig. 3(c) is the side grooved test piece having a side groove of 0.5 mm width and 3 mm depth on both sides of the standard 2 mmV-notch test piece[6].

Both of 22 mm and 50 mm thick specimens were sampled from the middle of the thickness (1/2 ht) of the weld zones and the base metal. The V-notch position of these specimens is the weld metal and bond (fusion boundary) for 22 mm thick and the weld metal, bond, and heat affected zone (HAZ: at 2 mm to the base metal side from melting boundary) for 50 mm thick plate.
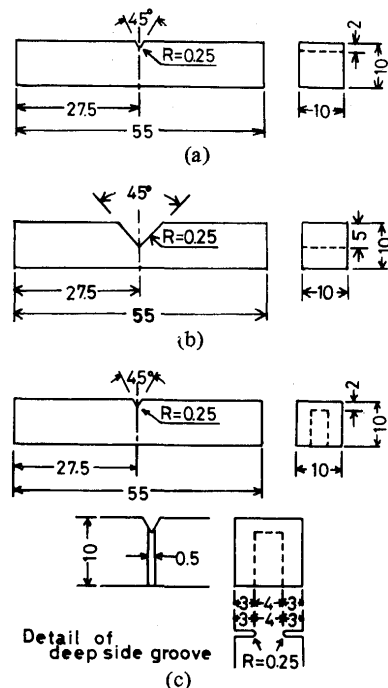

Fig. 3 Shapes of Charpy specimens used.
    (a) Standard 2 mmV-notch test piece
    (b) 5 mmV-notch test piece
    (c) Both-side deep grooved test piece

2.5 Measuring method of crystallinity

To find the crystallinity, the area of brittle fracture of the specimens after impact test was measured and the area was divided by the net sectional area of the specimens.

3. Test result and discussion

3.1 Influence of welding conditions on the shape of weld bead

To check the influence of welding heat input on the brittleness in single layer penetration welding, the specimens of 22 mm and 50 mm thickness were welded under various welding conditions.

Figure 4 shows the longitudinal and transverse cross sections and surface and back side appearance of the weld beads of 22 mm thick specimen when the welding heat input is reduced from Q = 19.1 kJ/cm to 7.5 kJ/cm.

To change the input heat, the welding speed (v_b) was set at 15, 30, 45 and 60 cm/minute under the constant beam voltage of V_b = 100 kV, and the beam current I_b, beam oscillation condition, and beam pass ratio $(\wp$ = pass current I_c/incident beam current I_b) were set at the optimum value respectively so that no internal defect such as porosity is produced at each welding speed.

At v_b = 15 cm/minute, the bead was shaped somewhat like a wedge and the bead width was about 4 mm in the middle of the plate thickness. At v_b = 30 cm/minute and over, the bead shape was approximately parallel and the bead width was reduced to about 2 mm.
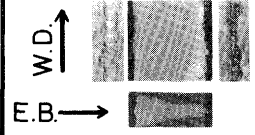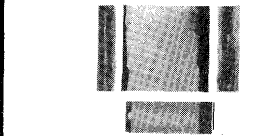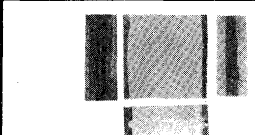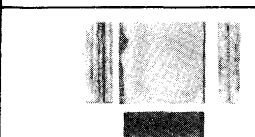
Figure 5 shows the cross sections of the fully penetrated bead of 50 mm thick specimen.

By setting the beam oscillation constant (frequency fx = 30 Hz, amplitude dx = 3 mm) and by changing the welding speed and the beam current, the heat input Q could be changed from 26 to 33 and 57 kJ/cm.

The bead shape was approximately parallel under each

condition and the bead width in the middle of the plate thickness was about 2 mm at Q = 26, 33 kJ/cm, and about 4 mm at Q = 57 kJ/cm.
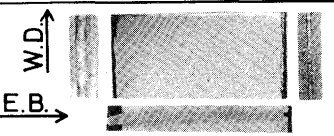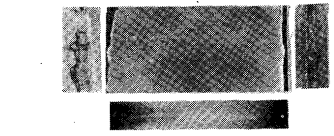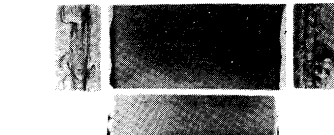
The obtained beads were sound without any crack or porosity.

Q (kJ/cm)	v_b (cm/min)	I_b (mA)	f_x (Hz)	$\wp$ (%)
19.1	15	53	10	10
12.6	30	70	30	10
10.8	45	90	30	10
7.5	60	100	100	25

V_b=100 kV, d_x= 3 mm, h_t=22 mm, SMK-50
① 0.16 wt% C (C_{eq} 0.333 wt%)

Fig. 4 Fully penetrated bead cross section and appearances of H.P.W. under various welding conditions (Plate thickness h_t = 22 mm)

	Heat input Q(kJ/cm)	Beam power Wb(kW)	I_b (mA)	v_b (cm/min)	$\wp$ (%)
	26			30	20
	33	16	160		30
	57	20	200	20	5

V_b = 100 kV f_x = 30 Hz d_x = 3 mm

Fig. 5 Fully penetrated bead cross sections and appearances of H.P.W. under various welding conditions (h_t = 50 mm)

3.2 Influence of heat input on structure and hardness of weld zones

For this test, specimens of 22 mm and 50 mm thick were welded while changing the welding heat input Q. To check the influence on the structure and hardness of the weld metal and bond, the heat input value in each case was converted into the heat input per unit plate thickness Q'.

Figure 6 shows the microstructures of weld metal and bond in the middle of the plate thickness when welded at the minimum and the maximum heat input per unit thickness, $Q' = 11.4$ kJ/cm^2 (Plate thickness $h_t = 50$ mm, $Q = 57$ kJ/cm, $v_b = 20$ cm/min), and $Q' = 3.4$ kJ/cm^2 ($h_t = 22$ mm, $Q = 7.5$ kJ/cm, $v_b = 60$ cm/min).

At $Q' = 11.4$ kJ/cm^2, the grain size are fairly coarse. At both weld metal and bond, the pro-eutectoid ferrite at grain boundary are turned to upper bainite structure inside grain, and M-A constituent is also seen partly between lathes.

At $Q' = 3.4$ kJ/cm^2, the grain size are fine, the weld metal is turned to lower bainite structure, and the bond to HAZ are turned to structure peculiar to electron beam welding as the result of quick heating and cooling. Namely, Diffusion of carbon in pearlite into ferrite is not sufficient in the welding thermal cycle and thus martensite of high carbon is seen at the parts which seem to be originally pearlite.

Figure 7 shows the Vickers hardness of the weld zones when heat input per unit thickness Q' is changed.

The hardness was measured at 1/2 plate thickness in the middle of the weld metal and of the bond. The hardness is lowered almost linearly as Q' increases. As described above, it was found that the structure and hardness of the weld zones change substantially depending on heat input by the one pass penetration welding up to 50 mm plate thickness.
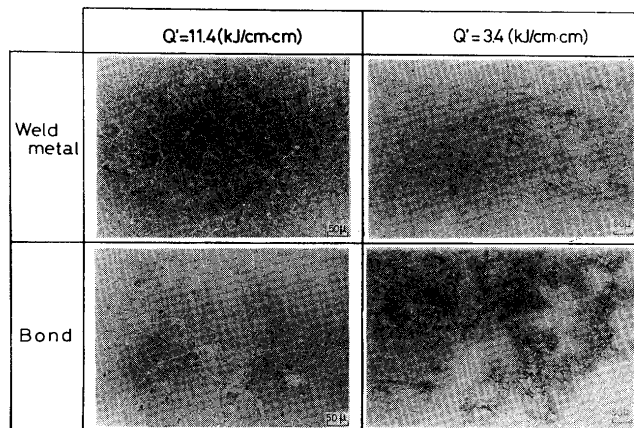

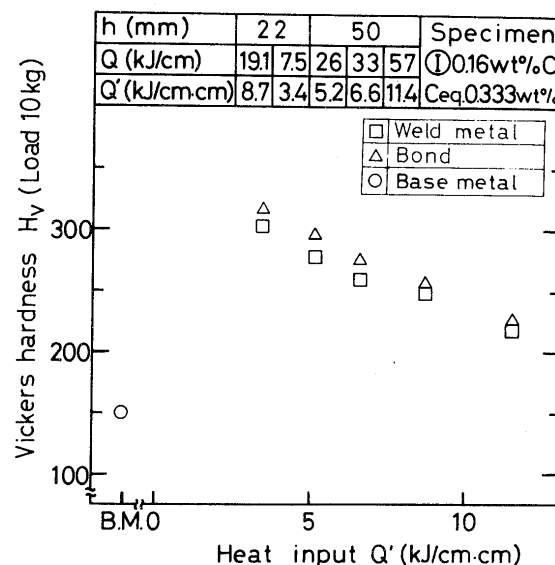| h (mm)	2 2		50			Specimen
Q (kJ/cm)	19.1	7.5	26	33	57	① 0.16wt%C
Q' (kJ/cm·cm)	8.7	3.4	5.2	6.6	11.4	Ceq.0.333wt%

□ Weld metal
△ Bond
○ Base metal

Fig. 7 Relation between maximum hardness and heat input for two position.

3.3 Impact property of electron beam weld zone

Charpy impact test is used populary to study toughness of electron beam weld zones as it is easy and economical. It is pointed out, however, that application of ordinary Charpy impact test of standard 2 mm V-notch to electron beam weld zone of narrow bead width results in a substantially different value of impact because of the difference in the break line of the test piece, i.e. the deviation from notch position[3),4),7)].

In this study, therefore, test pieces of 2 mm V-notch, 5 mm V-notch, and side grooved test piece were used for the Charpy impact test, and toughness was checked and evaluated through analysis of the property of these specimens.

(A) 2 mm V-notch test pieces Charpy impact test

Figure 8 shows the result of standard 2 mm V-notch Charpy impact test at 0°C of the weld zone of 22 mm thick test piece when the welding speed is changed.

The notch position is at the bond, and the measured energy absorption values are greatly dispersed compared with those of the base metal.

At $v_b = 15$ cm/minute, some are lower than the energy absorption of the base metal specified in JIS (2.8 kg-m: 0°C). At $v_b = 30$ cm/minute and over, however, all the values are over the JIS value. Dispersion in the values of absorbed energy is due to fracture paths deviated to HAZ and base metal side from the bond at the notch position as shown in **Fig. 9**.

The fracture is classified into three types of A, B, and C by the type of fracture path.

At observation of the fracture surface of the test piece, type A shows cleavage and thus brittle fracture on the

Fig. 6 Microstructures of weld metal and bond.

whole surface, type B shows both brittle and ductile fracture, and type C shows ductile fracture on the whole surface.

Figure 10 shows the result of Charpy impact test of the welds of 50 mm thick specimen with different heat input
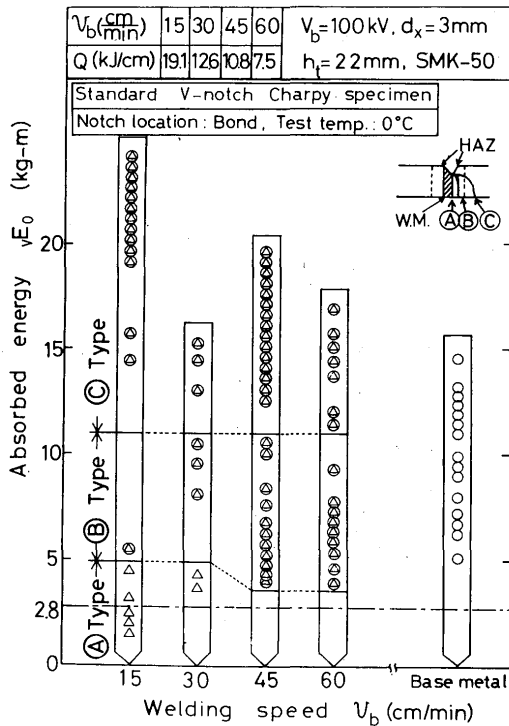

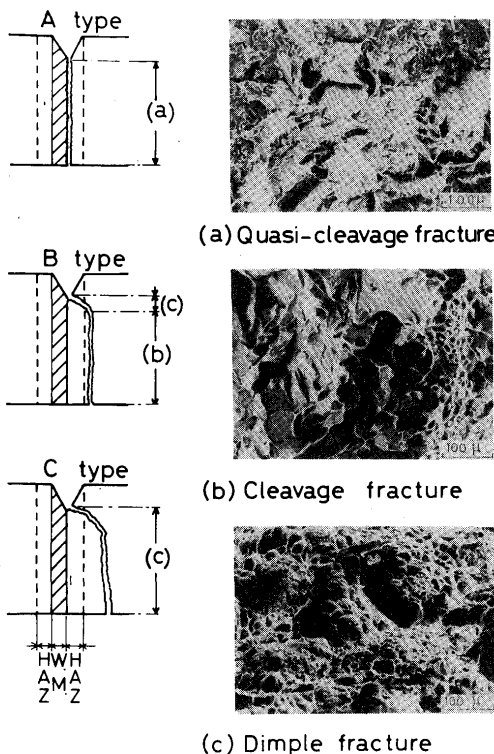Fig. 8 Results of Charpy impact test of welds at various welding speeds.

(a) Quasi-cleavage fracture

(b) Cleavage fracture

(c) Dimple fracture

Fig. 9 Schematic diagram of various fracture paths and fracture surfaces.

Q.

The notch position is at two places of weld metal center and bond, and the measured values of absorbed energy are greatly dispersed like in the case of 22 mm thick plate.

As the heat input increases to Q = 57 kJ/cm, some are lower than the specified value in JIS. When the bond is notched, the absorbed energy is lower than in the case of weld metal.

The above results of impact test indicates reduced heat input is effective for improvement of the toughness. It is difficult, however, to evaluate the toughness only with the standard 2 mm V-notch test pieces of this time which show great difference in fracture path and great scattering in the value of absorbed energy.

(B) 5 mm V-notch test pieces Charpy impact test

To minimize the defects of the standard 2 mm V-notch test, the test piece with 5 mm deep V-notch employed by Arata et al.[3] was used for the impact test.

Figure 11 shows the relationship between testing temperature and absorbed energy when the penetration welding is applied to 50 mm thick plate with heat input of Q = 33 kJ/cm and the Charpy test pieces with 5 mmV-notch on the weld metal, bond, and HAZ are used.

Compared with the case of the standard 2 mmV-notch, scattering of the data is less but fracture paths of those of higher absorbed energy and thus circled in the drawing are off the notch position. Except for those with deflected fracture path, the absorbed energy is higher in the order of bond, weld metal, and HAZ.

For relative comparison of these, the transition curve of the base metal was noted and the temperature showing 3.5 kg-m absorbed energy which is about a half of the shelf energy of the base metal, i.e. 3.5 kg-m absorbed energy ttansition temperature (vTE 3.5) was studied,
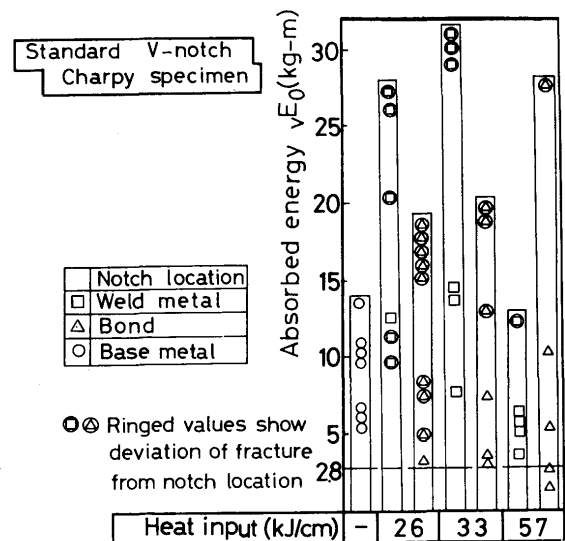

Fig. 10 Results of Charpy impact test of welds with different heat input (h_t = 50 mm).
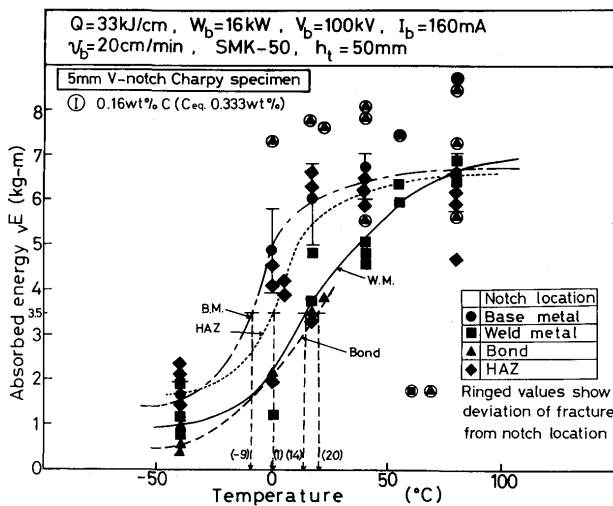
Fig. 11 Absorbed energy vs, temperature curves for 5 mmV-notch Charpy Specimens.

Fig. 12 shows the result. Like in the case of the standard 2 mmV-notch test piece, transition temperature of the base metal indicates similar tendency even by each notch position.

(C) Side grooved test pieces Charpy impact test

It was also tried to evaluate toughness of the material at a notched position by the information of the fracture surface after impact test i.e. crystallinity by using the standard 2 mm V-notch test piece with side grooves which is employed by Sato et al. for toughness evaluation[6].

Figure 13 shows temperature dependency of crystallinity in each notch position when side grooved Charpy test piece is used for the impact test. The fracture paths of all the test pieces were observed and those with more than 80% paths going off the noted material are circled for identification.

For toughness evaluation, comparison was made at the temperature of 50% crystallinity i.e. the fracture transition temperature (vT_S).

Figure 14 is to show vT_S in each heat input and each notch position and to compare with the base metal.
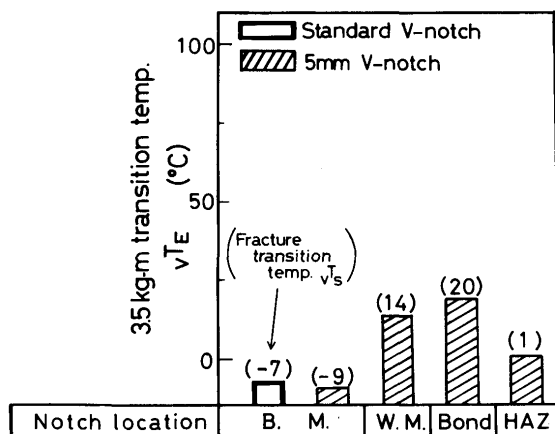

Fig. 12 Comparison of energy transition temperature vT_E and notch location of welds.
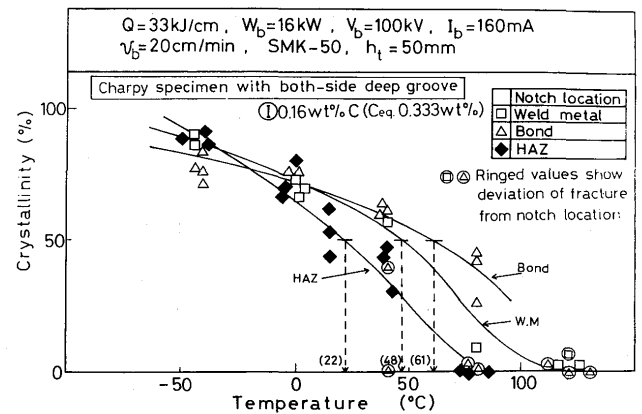

Fig. 13 Temperature dependency of crystallinity for Charpy specimens with both-side deep groove extracted from welds (h_t = 50 mm).

As heat input reduces, vT_S is lowered in the order of HAZ, weld metal and bond and the difference with the base metal (ΔT) tends to be lowered indicating improved toughness.

Figure 15 is to check the effect of heat input per unit thickness Q' on toughness and shows the relationship between Q' and vT_S.

As indicated, toughness of both weld metal and bond is improved substantially when Q' is reduced to 5 kJ/cm² and lower.

To check the cause of improvement toughness by small heat input, type of fracture surface on the test pieces was observed in each heat input per unit thickness and in each notch position.

Figure 16 shows SEM fractographs of the fracture surfaces of weld metal, bond and HAZ where the crystallinity is over 80% at heat input per unit thickness Q' of 6.6, 8.7, and 11.4 kJ/cm².

Both the weld metal and bond show a very large cleavage facture surface at heat input Q' mentioned above, and a river pattern is also seen. At the bond, the unit of fracture surface is getting larger as Q' increase than that of the weld metal. At the HAZ, however, the difference is not so significant.
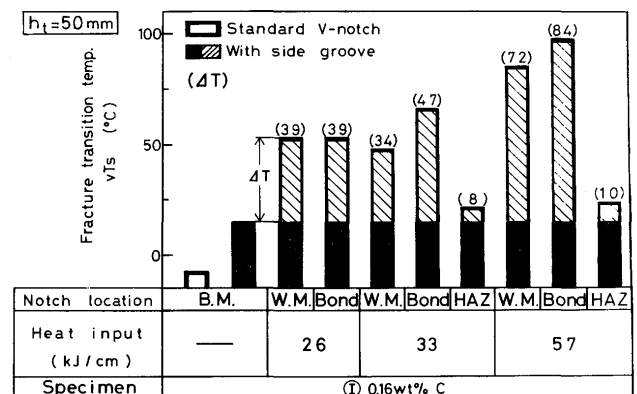

Fig. 14 Comparison of fracture transition temperature vT_S and heat input of Welds.

h_t(mm)	22		5 0			Specimen
Q(kJ/cm)	19.1	7.5	26	33	57	①0.16wt%C
Q'(kJ/cm·cm)	8.7	3.4	5.2	6.6	11.4	C$_{eq}$0.333wt%

O Standard V-notch
■▲● With side groove

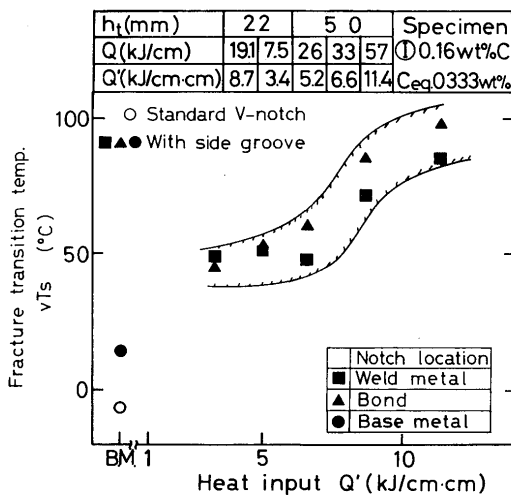| Notch location	
■	Weld metal
▲	Bond
●	Base metal

Fig. 15 Effect of heat input on fracture transition temperature of welds.

Figure 17 shows variation of fracture surfaces at the weld metal, bond, and base metal when Q' is reduced to 5.2 and to 3.4 kJ/cm^2.

The base metal shows cleavage fracture of comparatively small fracture unit but both of the weld metal and bond show quasi-cleavage fracture partly containing dimple fracture.

From the above observation, it turned out reduction in heat input makes the fracture unit smaller. Accordingly, correlation with structure was then studied.

Figure 18 show the microstructure along the fracture propagation path of brittle fracture surface at different input heat Q'. At Q' = 3.4 kJ/cm^2, the grain size is comparatively small in the martensite and lower bainite structures and the crack propagation distance short, which
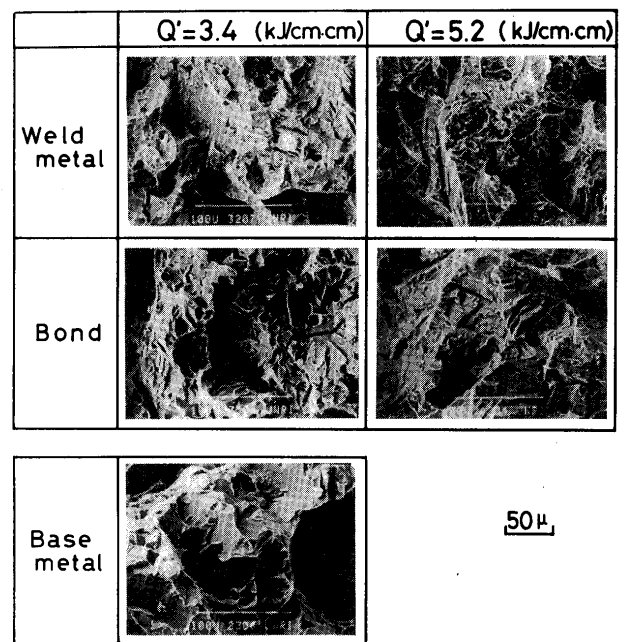

Fig. 17 Fractographs of Charpy impact test specimens.

prevents crack propagation and keeps toughness favorable.

When Q' is increased to 8.7 kJ/cm^2, it is turned into bainite structure and crack propagation distance becomes longer, which is considered to lower the toughness.

It is reported that M-A constituent[8] is produced as crystal grain size becomes coarse under the heat input condition where upper bainite structure is formed and the toughness is lowered[9],[10].

Figure 19 shows the microstructure and the SEM photo of the secondary crack, which seems to be the cause of broken M-A constituent. This is an magnified microstructure shown in Fig. 18.
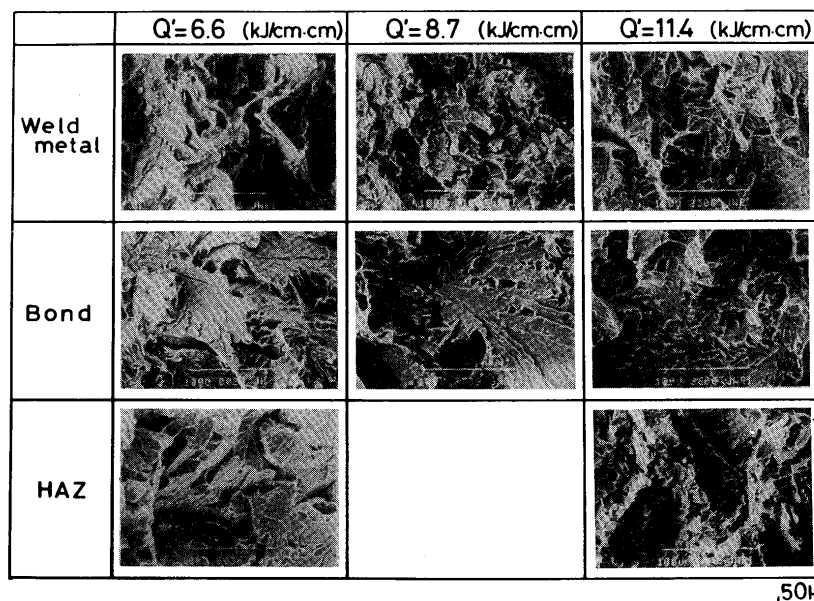

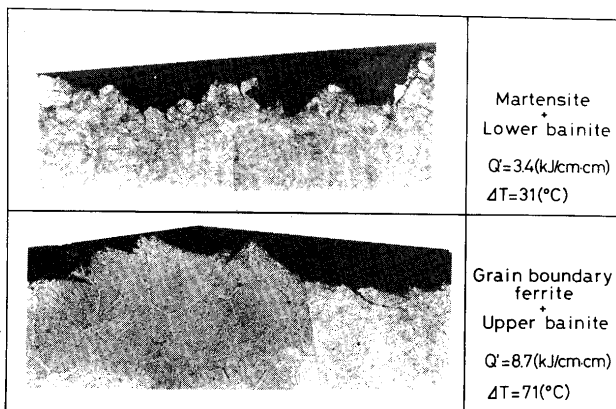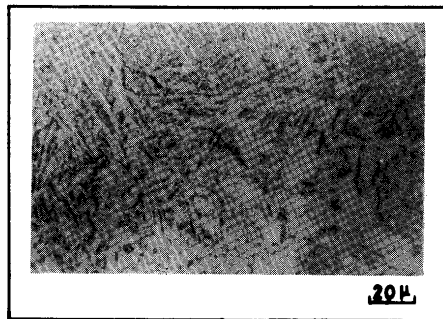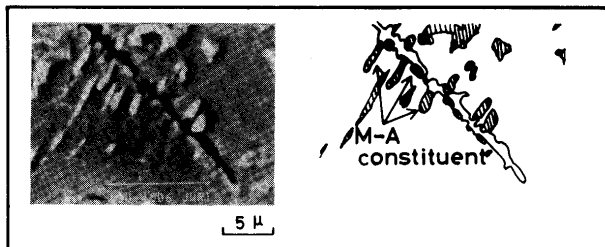Fig. 16 Fractographs of Charpy impact test specimens under various heat input Q'.

Fig. 18 Relation between the path of crack propagation and microstructure.
(Test temp.: −40°C, Charpy specimen with both-side deep groove).

(a)

(b)

Fig. 19 Example of secondary crack passing through the M-A constituent.
(a) Micrograph
(b) SEM micrograph and its schematic

4. Conclusions

With the specimens sampled from 50 kg/mm² class centrifugally cast steel pipe for welded structure and subjected to one pass horizontal full penetration electron beam welding, toughness of the welded zones was studied from the apects of welding heat input, micro structure and impact test properties. The obtained results are as summarized below.

1) At one-pass horizontal full penetration welding of 50 mm thick plate by 90° deflection horizontal electron beam, favourable beads of very narrow parallel shape with average bead width of 2 mm and without any internal defect could be obtained.

2) As the result of the micro structure observation of the

weld zones, both the weld metal and bond are transformed into upper bainite structure at high heat input in either case of 22 mm and 50 mm thick plates. When heat input is reduced, on the other hand, the weld metal is primarily transformed into lower bainite structure, and martensite is produced at the bond.

3) Through the analysis of the results of impact test using test pieces of the weld zones of different shapes, it turned out that the toughness is lowered as the heat input increases, and it tends to be lowered more at the bond than at the weld metal. In the case where the micro structure is transformed into upper bainite structure by large heat input, the causes for lowered toughness are the prior γ grains turned coarse, increased unit of fracture surface, and formation of M-A constituent.

At low heat input, the micro structure is transformed into martensite plus lower bainite and toughness is improved by finer prior γ grains, and reduced unit of fracture surface.

4) At the full penetration electron beam welding of thick plate of 0.16% carbon content, it turned out that the toughness is improved when the heat input per unit thickness Q′ is set at 5 kJ/cm² and lower. Practically, however, it is very difficult to lower the heat input below the minimum value of the test of this time. For toughness improvement, therefore, it will be necessary to study chemical composition of materials.

References

1) Y. Arata, M. Tomie, H. Han, H. Nishihara and T. Mihara: The Int. Conf. on Quality and Reliability in Welding, Sep. (1984), Hangzhou, China,; JWS Electron Beam Committee's Data EBW-288-82 (1982), (in Japanese).

2) J.A. Goldak and D.S. Nguyen: W.J., 2 (1977), 119-S.

3) Y. Arata, F. Matsuda, Y. Shibata, Y. Ono, M. Tamaoki and S. Fujihara: Trans. JWRI, 5 (1976), 27.

4) e.g. K. Satoh, M. Toyoda, K. Nohara, S. Takeda and M. Nayama: J. JWS, 51 (1982), 679 (in Japanese).

5) Y. Arata and M. Tomie: 2nd Int. Symp. JWS (1975),; Trans. JWRI, 4 (1975), 1: Trans. JWRI, 9 (1980), 157.

6) K. Satoh, M. Toyoda, F. Minami and K. Funato: Quarterly J. JWS, 3 (1985), 97 (in Japanese).

7) K. Seo and J. Masaki: J. JWS, 51 (1982), 291 (in Japanese).

8) Y. Nakao: J. JWS, 52 (1983), 235 (in Japanese).

9) H. Minura et al.: IIW, Doc. IX629-69 (1969).

10) M. Sato and K. Yamato: J. JWS, 50 (1981), 11 (in Japanese).